Metal kinetic-characteristic singularities due to the local geometry of the Fermi surface

G. T. Avanesyan, M. I. Kaganov, and T. Yu. Lisovskaya

Institute of High Temperatures, USSR Academy of Sciences
(Submitted 25 May 1978)
Zh. Eksp. Teor. Fiz. **75**, 1786–1800 (November)

The presence of parabolic points on the Fermi surfaces of metals leads to singularities in the angular dependence of the ultrasound absorption coefficient Γ_e when the sound propagates in the direction of the tangent to the parabolic point (Γ_e has a discontinuity or diverges logarithmically, depending on the local properties of the surface). At the same sound-propagation direction $\mathbf{k}/k$, a restructuring of the Pippard-oscillations takes place in a magnetic field $\mathbf{H}$ ($\mathbf{k}\perp\mathbf{H}$), and in some cases their amplitude should increase. The component $\Gamma_e(H)$, which depends monotonically on the magnetic field, has the same singularities as $\Gamma_e(0)$. The impedance singularities of the metal in the case of anomalous skin effect, which are due to parabolic points on the Fermi surface, are also considered.

PACS numbers: 72.55. + s, 71.25.Pi

1. INTRODUCTION

Collisionless interaction with a wave is experienced by those metal electrons whose velocity satisfies the Cerenkov condition

$$\mathbf{n}\mathbf{v}=s/v, \tag{1}$$

where $\mathbf{v}=v\boldsymbol{\nu}$ is the electron velocity, $\mathbf{s}=(\omega/k)\mathbf{n}$ is the phase velocity of the wave, ω is its frequency, and $\mathbf{k}=(\omega/s)\mathbf{n}$ is the wave vector. In metals at $\hbar\omega\ll\varepsilon_F$ and $T\ll\varepsilon_F$ (T is the temperature and ε_F is the Fermi energy), the principal role in the absorption of the wave energy is played by electrons located on the Fermi surface:

$$\varepsilon(\mathbf{p})=\varepsilon_F \tag{2}$$

($\mathbf{p}$ is the electron quasimomentum and $\varepsilon(\mathbf{p})$ is its energy).

We are interested below in the interaction between the electrons and the acoustic and electromagnetic waves. For sound $s\ll v_F$ [the subscript F denotes that we have in mind the Fermi electrons (2)]; for electromagnetic waves we confine ourselves to the case of strong spatial dispersion ($kv_F\gg\omega$). In either case, the condition (1) singles out the electrons whose velocity is almost perpendicular to the wave propagation direction $\mathbf{n}$. We shall frequently leave out completely the right-hand side of (1) and assume that

$$\mathbf{n}\mathbf{v}=0. \tag{1'}$$

The condition of interaction in the absence of collisions

$$kl\gg 1, \tag{3}$$

where $l=v_F\tau$ is the electron mean free path and τ is the time between the collisions, does not require satisfaction of the inequality $\omega\tau\gg 1$. It is possible that $\omega\tau\lesssim 1$ (see Refs. 1 and 2, as well as Appendix II of Ref. 3).

Equations (1) and (2) describe a line that passes over the Fermi surface. This line is frequently called a strip (and we shall henceforth use this term). If the Fermi surface is a sphere, then a change in the wave propagation direction changes neither the magnitude nor the structure of the strip (it passes along a "parallel" near the "equator," all that shifts is the position of the "pole"). In the case of an ellipsoid the topology of the strip does not change with changing $\mathbf{n}$, although its dimensions, of course, change. However, if the Fermi surface has depressions, necks, etc., then the situation changes in principle: When the wave propagation direction $\mathbf{n}$ changes, a structure of the strip and of its topology must of necessity change. We emphasize that the change of the structure of the strip is a general property of the metals. It appears that only in the case of Na, K, Cs, Rb, and Bi are the Fermi surfaces so simple that the topology of the strip does not depend on $\mathbf{n}$ (see Ref. 3, Appendix III).

We turn to two very simple but, as will be clear from the sequel, exhaustive examples of Fermi surfaces (see also Refs. 4–6). We consider strips on a Fermi surface of the dumbbell (or "dog bone") type, and on a Fermi surface of the type of corrugated plane (or "hilly locality"). They are shown in Figs. 1 and 2. It is seen from the figures that the topological structure of the strip remains unchanged until the direction of $\mathbf{n}$ coincides with some critical direction $\mathbf{n}_c$ ($\mathbf{n}_c=\mathbf{n}_X$ in Fig. 1 and $\mathbf{n}_c=\mathbf{n}_O$ in Fig. 2). In both cases, an entire cone of such directions exists. In the case of the dumbbell, at $\mathbf{n}=\mathbf{n}_X$ the belts coalesce at the points A and A', or else the belt breaks for "motion in the opposite direction" (Fig. 1). In the case of a corrugated plane at $\mathbf{n}=\mathbf{n}_O$ the belt degenerates to a point and vanishes. That the structure of the belt must change topologically in these cases is

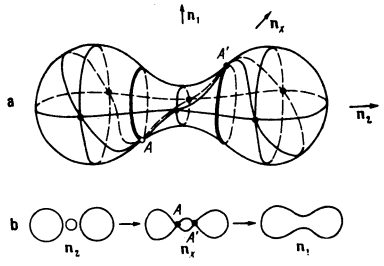

FIG. 1. a) Surface of the dumbbell ("dog bone") type. The thin lines denote the strips $\mathbf{n}\cdot\boldsymbol{\nu}=0$ [see (1')] and the thick ones strips of parabolic points; b) scheme showing the variation of the strip structure with changing orientation $\mathbf{n}$: $\mathbf{n}_2\to\mathbf{n}_X\to\mathbf{n}_1$.

 0038-5646/78/110900-08$02.40

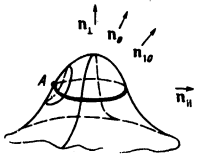

FIG. 2. Part of periodically repeating surface of the corrugated-plane type (or "hilly location" type). Strips [see (1′)] are shown corresponding to $\mathbf{n}=\mathbf{n}_{\parallel}$ and $\mathbf{n}=\mathbf{n}_{1O}$. At $\mathbf{n}=\mathbf{n}_{\perp}$ there is no strip, and at $\mathbf{n}=\mathbf{n}_O$ it degenerates into a point (point A). Thick line—strip of parabolic points.

clear from the figures. In Fig. 1 we have one strip at $\mathbf{n}=\mathbf{n}_1$ and three at $\mathbf{n}=\mathbf{n}_2$; when $\mathbf{n}$ goes continuously from $\mathbf{n}_2$ to $\mathbf{n}_1$, coalescence of the strips should take place. In Fig. 2 there is no strip at all at $\mathbf{n}=\mathbf{n}_{\perp}$ but there is one at $\mathbf{n}=\mathbf{n}_{\parallel}$; a direction should exist (between $\mathbf{n}_{\perp}$ and $\mathbf{n}_{\parallel}$) at which the strip is generated (vanishes).

The behavior of the families of strips at $\mathbf{n}\approx\mathbf{n}_c$ will be the subject of an analytic investigation (see Sec. 3). It is clear even now, however, that each critical strip (i.e., the strip at $\mathbf{n}=\mathbf{n}_c$) contains a singular point (or singular points): In the case of a dumbbell these are self-intersection points (points A and A' on Fig. 1), while in the case of a corrugated plane this is the point into which the strip degenerates (point A on Fig. 2). Self-intersection points will be called X-type points, and strip generation (vanishing) points will be called O-type.

Thus, each value of $\mathbf{n}_c$ corresponds to a definite singular point (or several points) on the Fermi surface. Its (their) determination is a geometrical problem whose solution calls for knowledge of the actual details of the Fermi-surface structure. At $\mathbf{n}\approx\mathbf{n}_c$ in the case of a point of O-type (for example, on a corrugated plane) the strip is an ellipse, and in the case of point of X-type (for example, on a dumbbell) the strip is approximated by segments of hyperbolas in the vicinity of the singular point (Fig. 3). If it is assumed that the strip singles out the electrons whose velocity is strictly perpendicular to the vector $\mathbf{n}$ [see (1′)], then the singular points (of X and O type) lie on the line of parabolic points[1)] of the Fermi surface, but if we start from Eq. (1), then the singular points lie near the line of the parabolic points. Figure 4 shows by way of example the Fermi surface of copper and the lines of the parabolic points are indicated. The location of the parabolic points on the Fermi surface is quite random, i.e., the direction of the unit normal ν to the Fermi surface at the parabolic point usually does not have high symmetry.

Points of any surface can be classified as 1) elliptic, 2) hyperbolic and 3) parabolic. Parabolic points can be of O-type or X-type. In addition, a degenerate type of parabolic points is possible. They are produced in the form of conical points or in the form of cylindrical sections on a surface. Points of this type are apparently extremely rare on the Fermi surfaces of metals. We shall not consider here parabolic points of the degenerate type.[2]

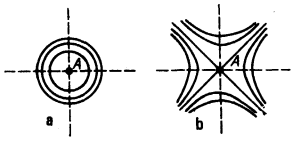

FIG. 3. Structure of strips $\mathbf{n}\cdot\nu=0$ at $\mathbf{n}\approx\mathbf{n}_c$: a) $\mathbf{n}\approx\mathbf{n}_O$, b) $\mathbf{n}\approx\mathbf{n}_X$.

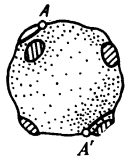

FIG. 4. Fermi surface of copper. The thick lines denote strips of parabolic points. A and A' are parabolic antipode points.

The purpose of the present communication is an investigation of the angular dependences, at $\mathbf{n}\approx\mathbf{n}_c$, of the absorption coefficient and velocity of sound (Secs. 2 and 3), and of the conductance tensor (Sec. 4). In Sec. 5 we examine the role of parabolic points when sound is absorbed in a magnetic field.

Concluding the introduction, we present an example of a closed Fermi surface cavity containing lines of parabolic points of both type—see Fig. 5. Similar cavities are possessed, for example, by the Fermi surfaces of platinum, cadmium, and chromium (Appendix III of Ref. 3).

2. SINGULARITIES OF THE SOUND ABSORPTION COEFFICIENT AT $T=0$, $\hbar\omega\to 0$, $kl\to\infty$

If the conditions listed in the section heading are satisfied, then the electronic part Γ_e of the sound absorption coefficient can be calculated with the aid of the formula[1]

$$\Gamma_e \approx \frac{2k\pi}{\rho(2\pi\hbar)^3}\oint\frac{dS}{v^2}|\Lambda|^2\delta\left(\mathbf{nv}-\frac{s}{v}\right), \tag{4}$$

in which the integration is over the Fermi surface, dS is the area element on the surface, and Λ is the corresponding component of the deformation potential. Λ depends on the polarization of the sound wave and on its propagation direction, but there are no grounds for expecting Λ to be anomalously small as a function of the quasimomentum at the parabolic points and (or) to have singularities at $\mathbf{n}\approx\mathbf{n}_c$.

The argument of the delta function vanishes, naturally, at the points of the strip (1). As already mentioned, at $\mathbf{n}=\mathbf{n}_c$ the strip degenerates into a point or has a self-intersection point. We assume the singular point on the strip of the Fermi surface to be given (we denote it by the letter A), and by the same token we assume given the critical propagation direction $\mathbf{n}_c$. We fix at the point

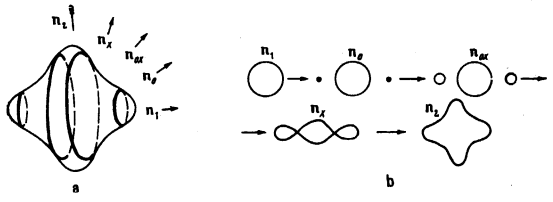

FIG. 5. a) Closed surface of "top" type. Lines of parabolic points of X and O type are shown (X-type—two large strips, O-type—two small ones). b) Schematic variation of the structure of the strip with changing direction of $\mathbf{n}$ from $\mathbf{n}_1$ to $\mathbf{n}_2$.

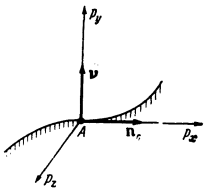

FIG. 6. Profile of Fermi surface near parabolic point. The origin is located at the parabolic point A. The p_y axis is directed along the outward normal ν to the Fermi surface. The p_x axis is tangent to the line of zero Gaussian curvature.

A an orthogonal coordinate system such that the plane $p_y=0$ is tangent to the Fermi surface at the point A, while the axes p_x and p_z lie in the principal sections of the surface[3] (see Fig. 6).

Assume (for simplicity) that the plane $p_z=0$ is a local-symmetry plane of the Fermi surface. Then, if a vector $\mathbf{n}$ close to $\mathbf{n}_c$ lies in the plane $p_z=0$, then the equation of the strip (1) takes the following form: In the case of an O-type point (see Fig. 3a)

$$|\alpha_x|p_x^2+|\alpha_z|p_z^2=\delta\theta, \quad \delta\theta=\theta-\theta_c, \tag{5}$$

and in the case of an X-type point (Fig. 3b)

$$|\alpha_x|p_x^2-|\alpha_z|p_z^2=\delta\theta, \quad \delta\theta=\theta-\theta_c; \tag{6}$$

α_x and α_z are in the general case quantities of the order of $1/p_F^2$ (see the next section); θ_c is an angle in the "laboratory" frame and corresponds to the critical direction $\mathbf{n}_c(A)$. The angle $\delta\theta=\theta-\theta_c$ ($|\delta\theta|\ll 1$) describes the deviation of the vector $\mathbf{n}$ from $\mathbf{n}_c\neq\mathbf{n}_c(A)$; $\delta\theta \approx [2(1-\mathbf{n}\cdot\mathbf{n}_c(A))]^{1/2}$. Near an O-type point, the strip exists only at $\delta\theta>0$, and near an X-type point the strip changes its topology at $\delta\theta=0$.

If $p_z=0$ is not a local-symmetry plane of the Fermi surface, then, for (5) and (6) to be valid, the vectors $\mathbf{n}$ and $\mathbf{n}_c(A)$ must be located in a plane making an angle to the plane $p_z=0$. When the vector $\mathbf{n}$ is close to $\mathbf{n}_c(A)$ but does not lie in the corresponding plane, then a point A_1 exists close to A and specifies the critical direction $\mathbf{n}_c(A)$ that is closest to $\mathbf{n}$ but does not coincide with $\mathbf{n}_c(A)$.

We shall show in this section that in the case of a point of O-type the value of Γ_e does not depend on $\delta\theta$ and is of the same order as for a larger strip, while the contribution of the region near a point of X type contains a large logarithmic factor, i.e., it exceeds (1) the contribution from the entire strip. These results serve as the foundation for the entire approach (see Sec. 3).

Substituting (5) and (6) in (4) we obtain for the singular part $\delta\Gamma_e$ of Γ_e in the case of an O-type point

$$\delta\Gamma_e^{(O)}=\frac{2k}{\rho}\frac{\pi^2|\Lambda_0|^2}{(2\pi\hbar)^3v_0^2|\alpha_x\alpha_z|^{1/2}}, \quad \delta\theta>0,$$
$$\delta\Gamma_e^{(O)}=0, \quad \delta\theta<0; \tag{7}$$

for an X-type point

$$\delta\Gamma_e^{(X)}(\theta)\approx\frac{2k\pi}{\rho}\frac{|\Lambda_0|^2}{(2\pi\hbar)^3v_0^2|\alpha_x\alpha_z|^{1/2}}\ln\frac{1}{|\delta\theta|}. \tag{8}$$

The superscript of Γ_e indicates the type of the singular point, and the quantities Λ_0 and v_0 are taken at the singular point (at $p_x=p_z=0$).

Comparison of the value of $\delta\Gamma_e^{(O)}$ (at $\delta\theta>0$) and of the coefficient at $\ln(1/|\delta\theta|)$ in $\delta\Gamma_e^{(X)}$ with the value[4] of Γ_e at $\mathbf{n}\neq\mathbf{n}_c$ demonstrates the validity of the statement made above concerning the role of the local vicinity of the singular points of O and X type. In addition, formulas (7) and (8) illustrate the character of the singularities of the electron part of the absorption coefficient of sound: An O-type point leads to a jump of Γ_e, and an X-type point leads to a logarithmic divergence.

3. ANALYTIC TREATMENT

As stated above, to avoid excessively cumbersome expressions, we chose from among the parabolic points one located in a local-symmetry plane of the Fermi surface. The choice of the coordinate system relative to the Fermi surface is clear from Fig. 6. Using the flattening of the surface at the parabolic point and the local symmetry of the Fermi surface with respect to p_z, it is convenient to write down the dispersion law in the vicinity of this point by expressing[5] p_y in terms p_x, p_z, and ε (the energy ε is reckoned from the Fermi surface):

$$p_y\approx\frac{\varepsilon}{v_0}-\frac{\varepsilon_{zz}}{2v_0}p_z^2-\frac{\varepsilon_{xy}}{v_0}\varepsilon p_x-\frac{1}{6}\frac{\varepsilon_{xxx}}{v_0}p_x^3+\ldots \quad (\varepsilon_{xxx}<0). \tag{9}$$

We have confined ourselves to the principal terms in the Taylor expansion in ε, p_z, and p_x; $v_0=\varepsilon_y(0,0,0)$; ε_i, ε_j, ε_{ijk} here and below are the partial derivatives of $\varepsilon(p)$ with respect to the components of the quasimomentum $\mathbf{p}$ at the parabolic point ($p_x=p_y=p_z=0$). The order of magnitude of the nonzero derivatives is estimated from dimensionality considerations (see footnote 4) and is the same for O and X points:

$$v_0\approx\frac{p_F}{m^*}; \quad \varepsilon_{ij}\approx\frac{1}{m^*}, \quad \varepsilon_{ijk}\sim\frac{1}{m^*p_F}, \quad \varepsilon_{zz}=0. \tag{10}$$

By definition, the velocity component is

$$\begin{aligned}v_x&=\varepsilon_{xy}p_y+{}^1/_2\varepsilon_{zzx}p_z^2+{}^1/_2\varepsilon_{yyx}p_y^2\\&\quad+\varepsilon_{xxy}p_xp_y+{}^1/_2\varepsilon_{xxx}p_x^2+\ldots,\\v_y&=v_0+\varepsilon_{yy}p_y+\varepsilon_{yx}p_x+{}^1/_2\varepsilon_{zzy}p_z^2\\&\quad+{}^1/_2\varepsilon_{yyy}p_y^2+\varepsilon_{yyx}p_yp_x+{}^1/_2\varepsilon_{xxy}p_x^2+\ldots,\\v_z&=\varepsilon_{zz}p_z+\varepsilon_{zzy}p_yp_z+\varepsilon_{zzx}p_xp_z+\ldots,\end{aligned} \tag{11}$$

and at the required calculation accuracy we get from (9)

$$\begin{aligned}\mathbf{n}\mathbf{v}&\approx\varepsilon_{xy}\varepsilon/v_0^2+w(\tilde p_x,p_z)+\delta\theta,\\w&=|\alpha_x|p_x^2+\alpha_zp_z^2,\end{aligned}$$

$$\alpha_x=\frac{1}{2v_0}\varepsilon_{xxx}, \quad \alpha_z=\frac{1}{2v_0}\left(\varepsilon_{zzx}-\frac{\varepsilon_{xy}\varepsilon_{zz}}{v_0}\right),$$

$$\tilde p_x=p_x-\frac{\varepsilon_{xy}^2-\varepsilon_{xxy}v_0}{\varepsilon_{xxx}v_0^2}\varepsilon. \tag{12}$$

The equation

$$w(\tilde p_x,p_z)=u$$

defines analytically a family of second-order curves—the ellipses or hyperbolas shown in Fig. 3. It is seen that the character of the singular point is determined by the sign of α_z, the expression for which contains the third derivatives of ε with respect to p_i; if $\alpha_z>0$, then the parabolic point is of the O type (Fig. 3a), and if $\alpha_z<0$ it is of the X type (Fig. 3b). The expansion (11) is justified by the fact that in the cases of interest to us $|u|\ll 1$.

Formulas (9) and (11) were obtained without additional assumptions concerning the properties of the Fermi surface. If for some reason the expansion $\mathbf{n}\cdot\boldsymbol{\nu}$ begins with higher powers of p_x and p_z, then the singularities observed should be sharper than those investigated in the present article.[6)]

The value $\mathbf{n}=\mathbf{n}_c$ at $\varepsilon=0$ corresponds to a singular strip (point $p_x=p_z=0$ for the O-type point and two intersecting straight lines for the X-type point).

An important role in what follows is played by the functions

$$\rho_\pm(u)=\frac{|\alpha_x\alpha_z|^{1/2}}{\pi}\int\int\frac{dp_x dp_z}{u\pm(\alpha_x p_x^2+\alpha_z p_z^2+i0)},\qquad |u|\ll 1, \tag{13}$$

whose singular parts do not depend on the parameters of the integration region. Designating by the symbol ∞ the equality of the singular parts, we obtain after elementary integration; for an O-type point ($\alpha_z>0$)

$$\rho_\pm^{(o)}(u)\infty\pm\ln(1/|u|)-i\pi\vartheta(-u), \tag{14}$$

where $\vartheta(x)=1$, $x>0$ and $\vartheta(x)=0$, $x<0$, and for an X-type point ($\alpha_z<0$)

$$\rho_\pm^{(x)}(u)={}^1/_2\pi\,\mathrm{sign}\,u-i\ln(1/|u|). \tag{15}$$

To calculate the singular parts of the sound-absorption coefficient and the frequency shift $\Delta\omega$, we use an expression obtainable in first-order perturbation theory if the sound wave is regarded as the cause of transitions in the electron gas[1]:

$$\Delta\omega-i\Gamma_e=\frac{2\omega}{\rho s^2(2\pi\hbar)^3}\int\frac{|\Lambda|^2\{n(\varepsilon)-n(\varepsilon+\hbar\omega)\}d^3p}{\varepsilon(\mathbf{p})+\hbar\omega-\varepsilon(\mathbf{p}+\hbar\mathbf{k})+i\hbar/\tau}. \tag{16}$$

Here Λ has the same meaning as in formula (4), and $n(\varepsilon)$ is the equilibrium Fermi function. Assuming the phonon momentum $\hbar k$ to be small, we can rewrite (16) in the form

$$\Delta\omega-i\Gamma_e\approx\frac{2}{\rho s(2\pi\hbar)_3}\int\frac{|\Lambda|^2}{v}\frac{\{n(\varepsilon)-n(\varepsilon+\hbar\omega)\}d^3p}{s/v(\mathbf{p})-\mathbf{nv}(\mathbf{p})+i/kl}. \tag{17}$$

Allowance for the next terms of the expansion of $\varepsilon(\mathbf{p}+\hbar\mathbf{k})$ in powers of $\mathbf{k}$ leads to a renormalization of the term $s/v(\mathbf{p})$ in the denominator of (17); this renormalization is quite inessential at $k\ll sm^*(v_F/s)^{1/2}$ (this condition in fact does not impose any limitations on the sound frequency).

As a result of the central symmetry of the electron dispersion law $\varepsilon(-\mathbf{p})=\varepsilon(\mathbf{p})$, each parabolic point on the Fermi surface has a point with antiparallel velocity (antipode point). If we start from the condition (1), then the antipode points correspond to the same value of the critical direction $\mathbf{n}_c=\mathbf{n}_{c'}$. In view of the allowance for the term s/v in the denominator of (17), the critical directions due to the antipode points differ somewhat from each other ($\mathbf{n}_c\neq\mathbf{n}_{c'}$). To limit the integration region to *the vicinity of one parabolic point*, we change over in (17) to integration over the half-space of the quasimomenta:

$$\Delta\omega-i\Gamma_e\approx\frac{2}{(2\pi\hbar)^3\hbar\rho s}\int\frac{|\Lambda|^2}{v}[n(\varepsilon)-n(\varepsilon+\hbar\omega)]\left\{\frac{1}{s/v(\mathbf{p})-\mathbf{nv}(\mathbf{p})+i/kl}+\frac{1}{s/v(\mathbf{p})+\mathbf{nv}(\mathbf{p})+i/kl}\right\}d^3p. \tag{18}$$

Using the chosen coordinate system (see Fig. 6) as well as expressions (11), we get

$$\frac{s}{v(\mathbf{p})}\mp\mathbf{nv}(\mathbf{p})+\frac{i}{kl}\approx\frac{s}{v_0}\mp\frac{\varepsilon_{xy}}{v_0^2}\varepsilon\mp(|\alpha_x|p_x^2+\alpha_z p_z^2+\delta\theta)+\frac{i}{kl}. \tag{19}$$

Substituting (19) in (18), we see that the singular parts of $\Delta\omega$ and Γ_e are determined only by the immediate vicinity of the singular point. As $kl\to\infty$ and $T\to 0$ we have

$$\Delta\omega-i\Gamma_e\infty\frac{2|\Lambda_0|^2\pi}{(2\pi\hbar)^3\rho\hbar s v_0^2}\int d\varepsilon[n_0(\varepsilon)-n_0(\varepsilon+\hbar\omega)]\left[\rho_+\left(\frac{s}{v_0}-\frac{\varepsilon_{xy}}{v_0^2}\varepsilon+\frac{i}{kl}+\delta\theta\right)+\rho_-\left(\frac{s}{v_0}+\frac{\varepsilon_{xy}}{v_0^2}\varepsilon+\frac{i}{kl}-\delta\theta\right)\right]. \tag{20}$$

Here $n_0(\varepsilon)$ is the Fermi step and

$$n_0(\varepsilon)-n_0(\varepsilon+\hbar\omega)=\begin{cases}0 & \text{at}\quad \varepsilon<-\hbar\omega,\ \varepsilon>0\\ 1 & \text{at}\quad -\hbar\omega<\varepsilon<0\end{cases}. \tag{21}$$

Expressions (20), (21), and (14) solve formally our problem of determining the singularities of $\Delta\omega$ and Γ_e. The arguments of the functions $\rho_\pm$ contain small parameters with different scales [see (10)]:

$$1\gg\frac{s}{v_0}\gg\max\left|\frac{\varepsilon\varepsilon_{xy}}{v_0^2}\right|=\frac{\hbar\omega|\varepsilon_{xy}|}{v_0^2}\approx\frac{s}{v_0}\frac{\hbar k}{p_F}. \tag{22}$$

This enables us to describe the singularities with different degrees of detail. We neglect the second term in the right-hand side of (19) and replace the difference (21) by a delta function. We then have

$$\Delta\omega-i\Gamma_e\approx\Gamma_e\left[\rho_+\left(\frac{s}{v_0}+\delta\theta\right)+\rho_-\left(\frac{s}{v_0}-\delta\theta\right)\right],\qquad \Gamma_e=\frac{2\pi^2|\Lambda_0|^2k}{(2\pi\hbar)^3\rho v^2|\alpha_x\alpha_z|^{1/2}}. \tag{23}$$

Figure 7 shows plots of Γ_e and $\Delta\omega$ against $\delta\theta$ for O and X points; these plots agree with (23), (14), and (15). From the presented formulas and from Fig. 7a it is seen that: 1) the singularity takes place at $\delta\theta_c=s/v_0$ and $\delta\theta_c=-s/v_0$, 2) a jump of the absorption coefficient Γ_e corresponds to a logarithmic singularity of $\Delta\omega$ while a jump of $\Delta\omega$ corresponds to a logarithmic singularity of Γ_e. As $s/v\to 0$ the singularities in $\Delta\omega$ vanish (the real parts of ρ cancel out), and the singularities of Γ_e are doubled (Fig. 7b).

Retaining in (19) the term that contains ε and integrating with respect to ε, we can determine the structures

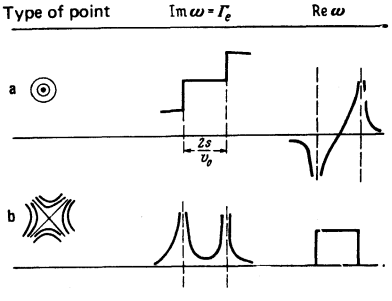

FIG. 7. Structure of angular singularities of Γ_e and $\Delta\omega$ for the cases of points of X and O type ($T=0$, $kl\to\infty$, $\omega\to 0$).

of the singularities described above: The jumps (of Γ_e and $\Delta\omega$) are replaced by jumps of the derivatives at the points $\pm s/v_0$ and $\pm s/v_0+\varepsilon_{xy}\hbar\omega/v_0^2$, and the logarithmic singularity is replaced by a singularity of the type $x\ln x$, with the maximum value of Γ_e (or $|\Delta\omega|$) of the order of $\Gamma_e\ln(\tilde{\varepsilon}/\hbar\omega)$, where $\tilde{\varepsilon}\approx\varepsilon_F$.

The fine structure of the singularities can be observed only under unique conditions; at $T\ll\hbar\omega$ and $kl\gg\varepsilon_F/\hbar\omega$. The finite temperature and the finite mean free path, naturally, smear out the singularities [see (18)]. If we assume for the sake of argument that the main smearing factor is the temperature (i.e., $T\gg\hbar/\tau$), then at $T\gg\hbar\omega$ the temperature smears out the jumps of Γ_e and $\Delta\varepsilon$ (the smearing width is $\sim T/\varepsilon_F$), and the maximum value of the logarithm in (14) and (15), meaning also (23), is $\ln(\varepsilon_F/T)$. At $T\ll\hbar\omega$ the weakened singularities are smeared out. Even at relatively high temperatures ($T\gg\hbar\omega$), when the directions $\delta\theta_c=s/v_0$ and $\delta\theta_{c'}=-s/v_0$ are indistinguishable (owing to the temperature smearing), the existence of parabolic points should manifest itself in an irregular $\Gamma_e=\Gamma_e(\theta)$ dependence; either an abrupt change (O-type) or a logarithmic increase (X-type) of the value of Γ_e in the interval $\delta\theta\sim T/\varepsilon_F$. Since $\Gamma_e\sim k$ [see (23)], the singularities (23) can be treated as singularities in the angular dependence of the sound velocity of the metal $s=s'-is''$ ($s''=\Gamma_e/k$).

4. SINGULARITIES OF THE CONDUCTANCE TENSOR

Starting from the Boltzmann kinetic equation in the τ approximation, we easily obtain an expression for the conductance tensor[1]:

$$\sigma_{ik}(\omega,\mathbf{k})=\frac{2e^2}{(2\pi\hbar)^3k}\oint_{\varepsilon(\mathbf{p})=\varepsilon_F}\nu_i\nu_k\frac{dS}{1/kl-i(\omega/kv_0-\mathbf{n}\mathbf{v})}. \tag{24}$$

The analysis of this expression is perfectly similar to the analysis of the expression for $\Delta\omega-i\Gamma_e$ (see (17) as $\hbar\omega\to0$). The main difference is that the numerator of the integrand contains the product of direction cosines—the normals to the Fermi surface $\nu_i\nu_k$, which make the singular parts of all the components, with the exception of σ_{yy}, very small or even zero (we use the required coordinate system, see Fig. 6). We shall therefore deal only with the component σ_{yy}, which is one of the transverse components of the tensor σ_{ik} and is significant in the investigation of the propagation of electromagnetic waves in a metal, and $\mathbf{n}_c=[1,0,0]$. In expression (24) the smearing factor is recognized to be the mean free path (it is assumed that $kl\ll\varepsilon_F/T$). Without repeating the analysis of the preceding section, we note the following:

1) The presence of an O-type point leads to a jump of $\mathrm{Re}\sigma_{yy}$ and to a logarithmic singularity in $\mathrm{Im}\sigma_{yy}$, where $|\mathrm{Im}\sigma_{yy}|\gg\mathrm{Re}\sigma_{yy}$. The component $\mathrm{Im}\sigma_{yy}$ has opposite signs at $\delta\theta=\delta\theta_c$ and $\delta\theta=-\delta\theta_{c'}$.

2) The presence of a point of X-type leads to a logarithmic increase of $\mathrm{Re}\sigma_{yy}$ and to a jump of $\mathrm{Im}\sigma_{yy}$. It seems just as possible to observe anomalies in the angular dependence of $\mathrm{Re}\sigma_{yy}$ as to observe analogous anomalies in the speed of sound and in its absorption coefficient, but the following must be borne in mind:

It is known from the theory of the anomalous skin effect that an electromagnetic wave attenuates in a metal as $l\to\infty$, i.e., $\mathrm{Im}k\neq0$. Therefore the singularities of σ_{yy} are smeared out even at $T=0$ and $l\to\infty$. According to the dispersion equation

$$k^3=4\pi i\sigma_{yy}(\omega,\ k)\omega/c^2, \tag{25}$$

we have as $l\to\infty$ [we omit a numerical factor of order unity in (25)]:

$$k'\approx k''\approx(\omega_0^2\omega/c^2v_F)^{1/3},\quad \omega_0^2=4\pi ne^2/m^*. \tag{26}$$

It is seen from (24) and (26) that the width $\Delta\theta$ of the smearing is determined by the following expression:

$$\Delta\theta\approx(\omega c/\omega_0v_F)^{2/3}. \tag{27}$$

The requirement $\Delta\theta\ll1$ does not impose any substantial limitations on the frequency. It must be borne in mind that in order for the formulas of this section to be valid it is necessary that the frequency ω satisfies the condition of the anomalous skin effect

$$\omega\tau\gg(\delta_0/l)^2,\quad \delta_0=c/\omega_0. \tag{28}$$

The logarithmic increase of $\mathrm{Im}\sigma_{yy}$ on account of O-type points leads to a curious situation wherein a weakly damped wave can propagate in a narrow angle interval. Indeed, according to the foregoing, wherever

$$\mathrm{Im}\,\sigma_{yy}<0,\quad |\mathrm{Im}\,\sigma_{yy}|\gg\mathrm{Re}\,\sigma_{yy},$$

the solution of the dispersion of the dispersion equation has the following structure ($l\to\infty$)

$$k'=\left(\frac{\omega_0^2\omega}{c^2v_F}\right)^{1/3}\ln^{1/3}\frac{k''v_F}{\omega},\quad k''=\frac{1}{3}\left(\frac{\omega_0^2\omega}{c^2v_F}\right)^{1/3}, \tag{29}$$

i.e.,

$$\frac{k'}{k''}=3\left[\frac{2}{3}\ln\frac{\omega_0v_F}{\omega c}\right]^{1/3}. \tag{30}$$

Observation of a weakly damped wave calls for satisfaction of a stringent requirement with respect to the direction of its propagation, and lowering the frequency [of course, within the limits of the inequality (28)] increases the ratio k'/k'', but decreases the region of accessible angles.

5. ROLE OF PARABOLIC POINTS IN THE ABSORPTION OF SOUND IN A MAGNETIC FIELD

It is known[7] that a sufficiently strong magnetic field $\mathbf{H}$ influences noticably the electronic absorption of sound by metals, and the character of this influence depends substantially on the value of $\mathbf{H}$ and on the relative positions of the vectors $\mathbf{k}$ and $\mathbf{H}$. We confine ourselves to intermediate fields

$$kl\gg kr_H\gg1,\quad r_H=cp_F/eH, \tag{31}$$

assuming that $\mathbf{k}\perp\mathbf{H}$. Then, according to Refs. 7 and 8, the sound absorption coefficient $\Gamma_e(H)$ is a sum of monotonic and oscillating parts:

$$\Gamma_e(H)=\Gamma_{\mathrm{mon}}+\Gamma_{\mathrm{osc}}. \tag{32}$$

We shall show that at $\mathbf{n}\approx\mathbf{n}_c$ both Γ_{mon} and Γ_{osc} should have characteristic singularities.

The monotonic part Γ_{mon} can be written in invariant form

$$\Gamma_{mon} \approx \frac{2k\pi}{\rho(2\pi\hbar)^3} \int \omega_c \tau \frac{|\Lambda|^2}{v^2} \delta(\mathbf{nv})\, dS, \tag{33}$$

where $\omega_c = eH/m^*c$, from which it is seen that Γ_{mon} has the same singularities as Γ_e at $H=0$.

We note that

$$\Gamma_{mon}(H) \sim \omega_c \tau \Gamma_e(0). \tag{34}$$

We proceed now to the oscillating part Γ_{osc} of the absorption coefficient. According to Ref. 7, the periods of the oscillations are given by

$$\Delta^{ij}\left(\frac{1}{H}\right) = \frac{2\pi e}{ck\Delta p_y^{ij}}, \tag{35}$$

where Δp_y^{ij} is one of the projections of the extremal (with respect to p_z) diameters that join the points (i, j) on the strip. When a line of parabolic points is present on the Fermi surface, the spectrum of the oscillations depends substantially on the direction of the vector $\mathbf{k} = k\mathbf{n}$. Figure 8 shows by way of example a Fermi surface on the dumbbell type, on which all the parabolic points of X type. It is seen that the number of periods is equal to four for some directions and to six for others.[7)]

On a surface of the top type (see Fig. 5), the change of the number of periods is connected not only with the break of the strip, which leads to departure of the strip from the extremal trajectory (X-type), but also with vanishing of the strip (O-type).

The amplitude of the oscillations is determined by the electrons located near the ends of the diameters. Therefore the influence of the flattening points of the Fermi surface is very substantial. It manifests itself in an angular dependence of the oscillation amplitudes.

Solution of the kinetic equation leads to the following expression for the sound absorption coefficient[7,8] ($\mathbf{k} \perp \mathbf{H}$, $\omega_c \tau \gg 1$):

$$\Gamma_{osc} = \frac{eH}{c(2\pi\hbar)^3\rho} \mathrm{Re} \iiint dp_z dt dt' \frac{\tau}{T} \Lambda(t) \Lambda^*(t') \times \exp\left\{ i \frac{kc}{eH} [p_y(t, p_z) - p_y(t', p_z)] \right\}, \tag{36}$$

where $T = 2\pi/\omega_c$, while t and t' are the times of motion on the electron trajectory in the magnetic field $\mathbf{H}$. The argument of the exponential contains the large parameter $\sim kr_H$. Therefore the main contribution to the integral is made by the stationary-phase points defined by the conditions

$$v_z^{ij} = \frac{c}{eH}\left(\frac{\partial p_y}{\partial t}\right)^{ij} = 0, \quad \left(\frac{\partial p_y}{\partial p_z}\right)^{ij} = 0. \tag{37}$$

The stationary-phase points (ij) are the points of intersection of the strip with the local-symmetry plane $p_z = \text{const}$. We assume that one of them (to be specific, the point i) is an ordinary elliptic point, and the other, j, is parabolic. Then, integrating in (36) with respect to t and t', we get according to Ref. 8

$$\Gamma_{osc}(H) = \frac{eH}{c(2\pi\hbar)^3\rho} \int dp_z \frac{\tau}{T} J_i J_j |\Lambda_i \Lambda_j| \times \mathrm{Re}\left[\exp\left\{ i\left(\frac{kc}{eH} \Delta p_y^{ij} - (\varphi_i - \varphi_j) + \frac{\varepsilon_{zz}}{2v_0} p_z^2 \right) \right\} \right], \quad \varepsilon_{zz} = \varepsilon_{zz}^i + \varepsilon_{zz}^j. \tag{38}$$

The amplitude and the phase of $\Gamma_{osc}(H)$ with period $\Delta^{ij}(1/H)$ are determined by the factors J_i and J_j, which depend on the structure of the Fermi surface near the points i and j. In our case the point i is elliptic and

$$J_i = \left| \int_{-\infty}^{\infty} \exp\{i\mathbf{kv}' t^2\} dt \right| = (2\pi/|\alpha_i|)^{1/2}, \quad \alpha_i = \mathbf{kv}_i,$$

and $\varphi_i = \pi/4$ if $\alpha_i > 0$ and $\varphi_i = -\pi/4$ if $\alpha_i < 0$ (assume, for the sake of argument, that $\alpha_i < 0$).

We change over to the variables p_z, ε, and t with the aid of the equations of motion

$$\frac{\partial p_z}{\partial t} = \frac{eH}{c} v_y, \quad \frac{\partial p_y}{\partial t} = -\frac{eH}{c} v_z. \tag{39}$$

Since[8)] $v_y = v_0 + O(p_z)$, it follows that $p_z \approx eHv_0 t/c + O(t^2)$ and

$$p_y(t, p_z) \approx p_y^j - \frac{\varepsilon_{zz}}{v_j} p_z^2 + \frac{1}{6}\left(\frac{eH}{c}\right)^3 v_j'' |\varepsilon_{zzz}^j| t^3 - \frac{eH}{c} t p_z^2 \alpha_{zj}. \tag{40}$$

Hence

$$J_j = \int_{-\infty}^{\infty} \exp\{i\beta_j t^3 - kv_j p_z^2 \alpha_{zj} t\} dt, \quad \beta_j = \mathbf{kv}/6 = ke^2H^2v_j''/6c^2 \sim kv_0\omega_c^2, \tag{41}$$

i.e., $\varphi_j = 0$ and consequently J_j is a real function.

If we use the Airy function

$$\mathrm{Ai}(\xi) = \frac{1}{2\pi} \int_{-\infty}^{\infty} \exp\left\{ \frac{i}{3} t^3 + \xi t \right\} dt,$$

whose asymptotic values are

$$\mathrm{Ai}(\xi) \sim \begin{cases} |\xi|^{-1/4} \sin(2/3 |\xi|^{3/2} + \pi/4), & \xi \to -\infty \\ \xi^{-1/4} \exp\{-2/3 \xi^{3/2}\}, & \xi \to +\infty \end{cases}, \tag{42}$$

then we can rewrite (41) in the form

$$J_j = \frac{2\pi}{(3\beta_j)^{1/3}} \mathrm{Ai}\left(-\frac{kv_j p_z^2 \alpha_{zj}}{(3\beta_j)^{1/3}} \right). \tag{41'}$$

When (38) is integrated with respect to p_z it must be recognized that the argument of the Airy function, which is of the order of $(kr_H)^{2/3} p_z^2/p_F^2$, is smaller by a factor $(kr_H)^{1/3}$ than the argument of the exponential. Consequently, in the vicinity of a stationary point the Airy function can be regarded as smoothly varying and be replaced by its constant value at the stationary point

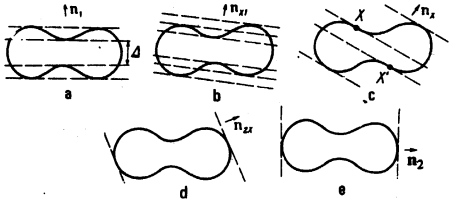

FIG. 8. Trajectory of motion of electron in coordinate space (Fermi surface of the dumbbell type). The dashed lines show the constant-phase planes of the sound wave, at the points of tangency with which of the Fermi surface the sound is effectively absorbed. $\Delta = c\Delta_F/eH$, where Δ_F is the corresponding characteristic distance in momentum space. a) Direction $\mathbf{n} = \mathbf{n}_1$—there are four periods, b) $\mathbf{n} = \mathbf{n}_{X1}$—six periods, c) $\mathbf{n} = \mathbf{n}_X$—four periods; d, e) directions $\mathbf{n} = \mathbf{n}_{2X}$ and $\mathbf{n}_2$—one period.

$\mathrm{Ai}(0)=3^{-1/6}\Gamma(1/3)2\pi$.

The oscillating part of the sound absorption coefficient at $\theta=\theta_c$ takes the form

$$\Gamma_{osc}^{ij}=A_{ij}\sin\left(\frac{kc}{eH}\Delta p_y^{ij}\right),$$
$$A_{ij}=\frac{eH\,\mathrm{Ai}(0)\,|\Lambda_i\Lambda_j|\tau}{c(2\pi\hbar)^3\rho(|\alpha_i|kc\varepsilon_{zz}/v_0eH)^{1/2}(3\beta)^{1/3}}. \tag{43}$$

In the usual case (j is an elliptic point)[8] we have

$$\Gamma_{osc}^{ij}\sim\Gamma_e\frac{\omega_c\tau}{(kr_H)^{1/2}}\sin\left(\frac{kc}{eH}\Delta p_y^{ij}+\frac{\pi}{4}\right). \tag{44}$$

From a comparison of expressions (43) and (44) we verify that since Δp_y^{ij} is based on an X-type point, the amplitude of the corresponding oscillation has an additional large factor $(kr_H)^{1/6}$. The phase of this oscillation differs from the ordinary one by $\pi/4$. Thus, in order of magnitude we have

$$\Gamma_{osc}^{ij}\approx\Gamma_e\frac{\omega_c\tau}{(kr_H)^{1/2}}. \tag{45}$$

If both i and j are parabolic X-type points (for example i is the antipode of the point j), then

$$\Gamma_{osc}^{ij}\approx\Gamma_e\frac{\omega_c\tau}{(kr_H)^{1/2}}\sin\left(\frac{kc}{eH}\Delta p_y^{ij}-\frac{\pi}{4}\right). \tag{46}$$

Compared with the case of two elliptic points, the amplitude of the absorption coefficient was increased by $(kr_H)^{1/3}$ times.

Let now the sound propagate in a direction tangent to an X-type point ($\mathbf{k}\perp\mathbf{H}$ as before), i.e., $\delta\theta\neq0$, with the sign of $\delta\theta$ corresponding to breaking of the strip ($\delta\theta>0$, see Fig. 9, strips a). At $p_z=0$ there are two close stationary-phase points, j and j'. Consequently, oscillations are produced with close periods. Their addition leads, naturally, to beats. At $\delta\theta\neq0$ we have in place of (40)

$$p_y=-\frac{\varepsilon_{zz}}{2v_0}p_z^2+\frac{1}{6}\left(\frac{eH}{c}\right)^3v_j^2|e_{zzz}^j|t^3-v_j\frac{eH}{c}t(p_z^2\alpha_{zj}+\delta\theta)+\ldots \tag{47}$$

and

$$J_j(\delta\theta)=\frac{2\pi}{(3\beta_j)^{1/3}}\mathrm{Ai}\left[-\frac{kv_j}{(3\beta_j)^{1/3}}(p_z^2\alpha_{zj}+\delta\theta)\right]. \tag{48}$$

The angular dependence of Γ_{osc}^{ij} is determined by the dependence of the argument of the Airy function on $\delta\theta$. It follows from (48) that at $\delta\theta\ll1/kr_H$ the integration with respect to p_z causes the dependence on $\delta\theta$ to vanish, and we return to (43). At $\delta\theta\gg1/kr_H$, after integrating with respect to p_z, we obtain

$$\Gamma_{osc}^{ij}\approx\Gamma_e\frac{\omega_c\tau}{(kr_H)^{1/2}}\mathrm{Ai}(-(kr_H)^{2/3}\delta\theta)\sin\left(\frac{kc}{eH}\Delta p_y^{ij}\right). \tag{49}$$

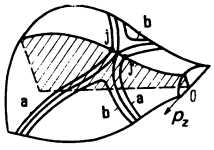

FIG. 9. Structure of strips at $\mathbf{n}\approx\mathbf{n}_c$ near the X point on the central section (shaded): a) break of strip and b) strip slips off the central section at a small deviation of $\mathbf{n}$ from $\mathbf{n}_c$.

We have retained the quantity $\delta\theta$ only where it enters with a large parameter $(kr_H)^{2/3}$. At a fixed magnetic field $\mathbf{H}$, according to (49), an oscillating dependence on $\delta\theta$ should be observed. The first maximum of the function $\mathrm{Ai}(\xi_m)$ is located near $\xi_1=-1.02$ (the first maximum of $\mathrm{Ai}(\xi_1)=1.16$).

Simple formulas can be obtained in the angle range $1\gg\delta\theta\gg1/(kr_H)^{2/3}$:

$$\Gamma_{osc}^{ij}\sim\Gamma_e\frac{\omega_c\tau\sin(2/3kr_H(\delta\theta)^{3/2}+\pi/4)}{(kr_H)^{1/2}\delta\theta^{1/4}}\sin\left(\frac{kc}{eH}\Delta p_y^{ij}\right). \tag{50}$$

At a fixed angle, beats should be observed with a period

$$\Delta_6\left(\frac{1}{H}\right)\sim\frac{3\pi e}{ckp_y}\frac{1}{|\delta\theta|^{3/2}}\gg\Delta^{ij}\left(\frac{1}{H}\right). \tag{51}$$

When the angle changes in the opposite direction ($\delta\theta<0$) the strip "slips off" the section $p_z=0$ (Fig. 9b) and the period is determined by the endpoints of the integration with respect to p_z ($p_z=\pm p_0=\pm|\delta\theta/\alpha_z|^{1/2}$). Using the saddle-point method in the integration with respect to p_z, we obtain for a function with a maximum at the end of the interval

$$\Gamma_{osc}^{ij}(\delta\theta)=\frac{eH}{c(2\pi\hbar)^3\rho|\alpha_i|^{1/2}|(3\beta_j)^{1/3}|}$$
$$\times\int_{\sqrt{|\delta\theta/\alpha_z|}}^{p_E}\frac{\tau}{T}|\Lambda_i\Lambda_j|\mathrm{Re}\exp\left\{i\frac{kc}{eH}\frac{\varepsilon_{zz}}{2v_j}p_z^2\right\}\mathrm{Ai}\left[-\frac{kv_0}{|(3\beta_j)^{1/3}|}(\delta\theta+p_z^2\alpha_z)\right]dp_z$$
$$\sim\frac{A_{ij}}{\mathrm{Ai}(0)}\mathrm{Re}\int_0^\infty\frac{\exp\{i[y+kr_H\delta\theta]\}\mathrm{Ai}(y(kr_H)^{-2/3})}{(y+|\delta\theta|kr_H)^{1/2}}dy. \tag{52}$$

The Airy function can be regarded as a smooth function in the vicinity of $y\lesssim1$ and replaced by its value at zero. We can therefore express Γ_{osc}^{ij} in terms of Fresnel integrals and write down in explicit form the asymptotic expressions

$$\Gamma_{osc}^{ij}(\delta\theta)\sim A_{ij}\left[1-\left(\frac{kr_H|\delta\theta|}{\pi}\right)^{1/2}\sin\left(\frac{kc}{eH}\Delta p_y^{ij}\right)\right.$$
$$\left.+\left(\frac{kr_H}{\pi}|\delta\theta|\right)^{1/2}\cos\left(\frac{kc}{eH}\Delta p_y^{ij}\right)\right]\quad\text{at}\quad|\delta\theta|\ll\frac{1}{kr_H};$$
$$\Gamma_{osc}^{ij}(\delta\theta)\sim\frac{\Gamma(0)}{(kr_H)^{1/2}|\delta\theta|}\quad\text{at}\quad\delta\theta\gg\frac{1}{kr_H}. \tag{53}$$

Attention should be called to the fact that with increasing $\delta\theta$ the amplitude of the oscillations decreases and vanishes at a certain angle value that depends on the shape of the Fermi surface.

In the case of O-type points, the amplitude decrease due to the vanishing of the strip at $\theta=\theta_c$ begins with $\delta\theta\lesssim1/kr_H$ (the amplitude decreases like $(kr_H|\delta\theta|)^{1/2}$. At $|\delta\theta|>1/kr_H$ the picture of the Pippard oscillation is similar to the X-type points at $1\gg\delta\theta>0$ [formulas (49)–(51)].

CONCLUSION

The anomalous angular dependences of the sound absorption coefficient and of the electric conductivity tensor, predicted in this article, can be observed without satisfying particularly stringent conditions on the frequency, magnetic field, or mean free path. We see only one difficulty in the need of studying the spatial waves in a direction that is random with respect to the crys-

tallographic axes. It is possible that it is this difficulty which explains why no such anomalies were observed so far.

In conclusion, we take the opportunity to thank I. M. Lifshitz and L. P. Pitaevskiĭ for stimulating discussions.

[1)]The lines of parabolic points are the border lines between Fermi-surface sections having Gaussian curvatures of opposite sign. At the parabolic point, one of the principal curvatures of the surface reverses sign. A parabolic point is a point where the surface flattens.

[2)]The propagation and absorption of sound in metals whose Fermi surfaces contain degenerate parabolic points were considered in Refs. 5 and 6 with chalcogenides as examples.

[3)]The critical-direction cone can be constructed by moving along a line of parabolic points.

[4)]In the case of a spherical Fermi surface, assuming that Λ does not depend on the angles, we easily obtain from (4)

$$\Gamma_e = \frac{2k|\Lambda|^2\pi^2 p_F^2}{\rho(2\pi\hbar)^3 v_F^2} = \frac{2k|\Lambda|^2\pi^2(m^*)^2}{\rho(2\pi\hbar)^3}, \quad m^* = \frac{p_F}{v_F}.$$

If we assume $\Lambda \approx p_F^2/m^*$, $p_F \approx \hbar/a$, $\rho \approx M/a^3$, $m^* \approx m_0$ (m_0 is the mass of the free electron, M is the mass of the ion metal, and a is the interatomic distance), and $s^2 = (m_0/M)v_F^2$, then $\Gamma_e/\omega \approx (m_0/M)^{1/2}$. This is only an order-of-magnitude equality, and it determines the scale of the electronic part of the sound absorption coefficient.

[5)]In this system the coordinates of the parabolic point are $p_x = p_z = 0$ and $\varepsilon = 0$.

[6)]This is most unlikely, since the parabolic points do not have high symmetry (see above, as well as Ref. 6).

[7)]It is seen from the very same figure that at certain directions of $\mathbf{n}$ ($\mathbf{n}_1$ in the figure) the number of periods can decrease because of the symmetry of the Fermi surface, which causes some extremal diameters to coincide.

[8)]We measure p_z from that value at which $\Delta^{ij}p_y(p_z)$ has an extremum.

[1]A. I. Akhiezer, M. I. Kaganov, and G. Ya. Lyubarskiĭ, Zh. Eksp. Teor. Fiz. 32, 837 (1957) [Sov. Phys. JETP 5, 685 (1957)].
[2]M. Ya. Azbel' and M. I. Kaganov, Dokl. Akad. Nauk SSSR 95, 41 (1954).
[3]I. M. Lifshitz, M. Ya. Azbel', and M. I. Kaganov, Élektronnaya teoriya metallov (Electron Theory of Metals), Nauka, 1971.
[4]G. T. Avanesyan, M. I. Kaganov, and T. Yu. Lisovskaya, Pis'ma Zh. Eksp. Teor. Fiz. 25, 381 (1977) [JETP Lett. 25, 355 (1977)].
[5]V. M. Kontorovich and N. A. Sapogova, Pis'ma Zh. Eksp. Teor. Fiz. 18, 381 (1973) [JETP Lett. 18, 223 (1973)].
[6]N. A. Stepanova, Fiz. Nizk. Temp. 3, 1415 (1977) [Sov. J. Low Temp. Phys. 3, 680 (1977)].
[7]A. B. Pippard, Philos. Mag. 46, 1104 (1955).
[8]V. L. Gurevich, Zh. Eksp. Teor. Fiz. 37, 71 (1959) [Sov. Phys. JETP 10, 51 (1960)].

Translated by J. G. Adashko

Symmetry of "current" states and spontaneous oscillations in bismuth

G. I. Babkin, V. T. Dolgopolov, and P. N. Chuprov

Institute of Solid-State Physics, Academy of Sciences of the USSR, Moscow

(Submitted 30 May 1978)
Zh. Eksp. Teor. Fiz. **75**, 1801–1811 (November 1978)

Irradiation of a metal plate with radio waves may produce a macroscopic magnetic moment in zero magnetic field, i.e., it may induce a transition to a "current" state. A calculation is given of the width and position of hysteresis loops which appear because of the induced magnetic moment. A study is made of the stability of the current states and it is shown that—under certain conditions—periodic oscillations of the magnetic moment may be expected. A report is given of measurements carried out on bismuth in which such spontaneous oscillations were observed experimentally.

PACS numbers: 78.70.Gq, 75.60.Ej, 75.70.Kw

Irradiation of a metal plate with radio waves may produce a macroscopic magnetic moment because of rectification of the rf current.[1,2] The inequivalence of two consecutive half-periods of the rf current is due to the presence of a static magnetic field. When the magnetic field created by the rectified current itself is sufficient to maintain the rectification process, a sample retains a magnetic moment even in zero magnetic field. A metal can then assume at least two "current" states which differ in respect to the direction of the rectified current and, consequently, in respect to the sign of the magnetic moment of the sample. Application of an external magnetic field anti-parallel to the magnetic moment causes a sudden transition from one current state to the other. The dependence of the magnetic moment on an external magnetic field in the presence of an additional large-amplitude alternating field exhibits a hysteresis loop. This behavior has been observed experimentally and investigated in bismuth and tin.[1,2]

The rectification mechanism, which produces such current states, was proposed by us earlier.[3] In one of the half-periods of the alternating field when the external magnetic field is antiparallel to the alternating field, an open trajectory shown in Fig. 1b appears near the surface. Electrons moving along this trajectory enter more frequently the skin layer than those moving

 0038-5646/78/110907-06$02.40